# Validation of Atmospheric Infrared Sounder temperature and moisture profiles over tropical oceans and their impact on numerical simulations of tropical cyclones

Zhaoxia Pu[1] and Lei Zhang[1]

Received 25 March 2010; revised 20 September 2010; accepted 15 October 2010; published 23 December 2010.

[1] The quality of the retrieved temperature and moisture profiles acquired from the Atmospheric Infrared Sounder (AIRS) aboard the NASA Aqua spacecraft was evaluated by comparing the data with dropsonde observations obtained from NASA African Monsoon Multidisciplinary Analyses (NAMMA 2006) and international THORPEX Pacific Asian Regional Campaign (T-PARC 2008) field programs. Results indicate that the AIRS retrieved temperature profiles are in good agreement with dropsonde observations. However, the AIRS retrieved moisture profiles show a larger bias compared with the dropsondes over the tropical oceans where tropical cyclones developed. A series of data assimilation experiments is then performed with an advanced research version of the Weather Research and Forecasting model and its three-dimensional variational data assimilation system. Results show that the assimilation of the AIRS retrieved temperature and moisture profiles has a significant impact on the numerical simulations of tropical cyclones. However, the overall impacts of the data assimilation on numerical simulations of tropical cyclones are very sensitive to the bias corrections of the data. Specifically, the dry biases of moisture profiles cause the decay of Tropical Storm Debby (2006) in the numerical simulations. Only with bias correction can data assimilation result in a reasonable portrayal of storm development. Compared with the moisture profiles, temperature profiles show a larger impact on the track forecasting. Assimilation of the temperature profiles resulted in significant improvements in the track forecasts for both Debby (2006) and Typhoon Jangmi (2008).

**Citation:** Pu, Z., and L. Zhang (2010), Validation of Atmospheric Infrared Sounder temperature and moisture profiles over tropical oceans and their impact on numerical simulations of tropical cyclones, *J. Geophys. Res.*, *115*, D24114, doi:10.1029/2010JD014258.

## 1. Introduction

[2] Tropical cyclones are one of the costliest and deadliest natural disasters in the United States and other countries around the world. The accurate forecast of the formation, evolution and intensity change of tropical cyclones is of great importance in issuing proper warnings to the public, and thus decreasing the potential for economic damage and deaths. However, due to the lack of the conventional observations over the oceans, deficiencies in model initial condition can lead to inaccurate tropical cyclone forecasts in modern numerical weather prediction.

[3] With advancements in remote sensing techniques, the amount of usable satellite data has increased rapidly in the last 2 decades. Many satellite derived data products have become useful sources for hurricane analysis and forecasting. Early studies by *Velden et al.* [1998], *Leslie et al.* [1998], and *Soden et al.* [2001], and the recent studies by *Zhang et al.* [2007] and *Pu et al.* [2008], all indicate that satellite wind data derived from the Geostationary Operational Environmental Satellites (GOES) has a significant impact on hurricane track forecasting. *Hou et al.* [2000] assimilated the SSM/I and TRMM Microwave Image (TMI) derived surface rainfall and total precipitatble water into the NASA Goddard Earth Observing System (GEOS) global analysis with a one-dimensional variational data assimilation (1DVAR) minimization procedure. They demonstrated that the assimilation of the TMI and SSM/I satellite rainfall rates results in improvements in hurricane track forecasts in the GEOS global model [*Hou et al.*, 2004]. With the fifth-generation Pennsylvania State University-National Center for Atmospheric Research Mesoscale Model (MM5), *Pu et al.* [2002] found that the TMI rain rate had a significant impact on the mesoscale numerical simulation of Supertyphoon Paka (1997). *Chen* [2007] demonstrated the positive impact of QuikSCAT and SSM/I derived satellite wind on the numerical simulation of Hurricane Isidore (2002). In a recent study, *Pu et al.* [2008] showed that the wind data derived from the GOES-11 rapid scan and QuikSCAT satellite improved the qualitative precipitation forecasting associated with two storms near landfall.

[1]Department of Atmospheric Sciences, University of Utah, Salt Lake City, Utah, USA.


0148-0227/10/2010JD014258

[4] Although most of the aforementioned satellite wind and precipitation data show a positive impact on the numerical simulation and prediction of a hurricane, most of them are not able to represent the vertical structure of the atmosphere. In other words, the atmospheric profile information was generally lacking before the Advanced Microwave Sounding Unit (AMSU) and the Atmospheric Infrared Sounder (AIRS) were launched into orbit.

[5] As part of NASA's Earth Observing System (EOS) mission, the AIRS and its companion AMSU-A were launched into polar orbit onboard the NASA Aqua Satellite in May 2002. The primary scientific achievements of AIRS are to study the global water and energy cycle [*Tian et al.*, 2006] and to improve the weather prediction [*Le Marshall et al.*, 2005a, 2005b]. Specifically, AIRS retrieved products include the temperature and moisture (water vapor mixing ratio) profiles. By generating information on the vertical structure of the atmosphere, AIRS sensor provides an excellent opportunity to examine the impact of atmospheric thermodynamic variables on the simulation and prediction of tropical cyclones.

[6] The results of assimilating AIRS data in the global models showed that the data were helpful for improving the skill of numerical simulation and forecasts. Specifically, the assimilation of AIRS data has been achieved by assimilating AIRS retrieved products or the direct assimilation of satellite radiances. Using AIRS retrieved clear-sky temperature and humidity profiles, *Atlas* [2005] found a positive impact from the AIRS retrieved temperature profiles in the NASA's finite volume general circulation model (FVGCM) with the NOAA National Centers for Environmental Prediction (NCEP) spectral statistical interpolation (SSI) analysis system, particularly in the Southern Hemisphere. *Wu et al.* [2006] have also shown similar improvements in hurricane mesoscale simulations. By assimilating quality-controlled AIRS temperature retrievals under partially cloudy conditions, *Reale et al.* [2008] have shown the positive impact of AIRS retrieved temperature on the analysis and track prediction of tropical cyclone Nargis, which devastated Myanmar (formerly Burma) in May 2008 using a high-resolution version of NASA GEOS-5 global assimilation and analysis system. In addition to the AIRS retrievals, both NCEP and European Centre for Medium Range Weather Forecasting (ECMWF) have reported improvement in the operational forecast due to the assimilation of clear-sky AIRS radiances data [*Pavelin et al.*, 2008].

[7] While most of the previous studies mainly demonstrated the impact of AIRS clear sky radiances or quality-controlled (subset of selected data) retrievals (temperature profiles) on numerical simulation and prediction, there has not yet been a clear consensus regarding how AIRS data should be properly assimilated. There has been much controversy concerning the effectiveness of the direct assimilation of satellite radiances versus the assimilation of satellite retrievals. *Derber and Wu* [1998] conclude that the direct assimilation of satellite radiances resulted in better forecasts compared with the outcomes from the assimilation of retrievals. However, according to *Joiner and Dee* [2000], many of the studies showing improvement may also be overlooking changes introduced simultaneously with the direct assimilation system, such as changes in the quality control and systematic error correction algorithms. Despite the advantages and disadvantages of each method, most current applications assimilate satellite radiances or retrieved products under clear-sky conditions. The direct assimilation of satellite radiances under cloudy and precipitating conditions is still a challenging problem that has received large attention from the community [*Errico et al.*, 2007]. Therefore, in order to study severe weather systems, such as tropical cyclones (where the cloud and precipitation effects cannot be ignored), the use of retrieved products is a preferred way of assimilation simply because the retrieved data are available. However, over the cloudy and precipitating areas, errors in these retrieved data are expected to be large. Therefore, before assimilating AIRS retrieved data products, such as temperature and moisture profiles into numerical models, the overall quality of the data should be evaluated.

[8] Most previous studies have emphasized the evaluation of the impact of temperature retrievals; not enough attention was given to the retrieved moisture profiles. Therefore, the objective of this study is to evaluate overall quality of AIRS retrieved temperature and moisture profiles over the tropical oceans near the tropical cyclone environment. Specific attention will be given to the quality and impact of the AIRS moisture profiles on the tropical cyclone forecast. Particularly, we will first evaluate the quality of AIRS retrieved profiles by comparing the data with the dropsonde observations collected during NASA African Monsoon Multidisciplinary Analyses (NAMMA; August to September 2006) over the eastern Atlantic Ocean and the THORPEX Pacific Asian Regional Campaign (T-PARC, August to October 2008) over the western Pacific Ocean, both near tropical cyclone environments. With arbitrarily selected tropical cyclone cases, the influence and *relative* importance of atmospheric temperature and moisture profiles on the numerical simulations of tropical cyclone formation and intensification are evaluated. The quality and biases of the data, the influence of the bias correction of the AIRS retrieved temperature and moisture profiles on data assimilation and their impact on numerical simulations of tropical cyclones are also examined. An advanced research version of the mesoscale community Weather Research and Forecasting (an Advanced Research WRF or ARW) model [*Skamarock et al.*, 2008], developed at the National Center for Atmospheric Research (NCAR), and its three-dimensional variational data assimilation (3DVAR) system [*Barker et al.*, 2004a, 2004b] are used.

[9] The paper is organized as follows: Section 2 describes the results of comparison between the AIRS retrieved temperature and moisture profiles and the dropsonde observations from both NAMMA and TPARC field programs. Section 3 examines the impact of the AIRS moisture and temperature profiles on tropical cyclone forecasts. The sensitivity of tropical cyclone forecast to the bias correction of the data is also discussed. Concluding remarks are made in section 4.

## 2. Comparison of AIRS Temperature and Moisture Profiles With Dropsonde Data From NAMMA and T-PARC Field Experiments

### 2.1. AIRS Data

[10] The NASA AIRS is the most advanced and sophisticated spaceborne atmospheric profiler [*Aumann et al.*, 2003]. AIRS is one of six instruments on board the NASA Aqua spacecraft, and has been operational since September 2002. It is accompanied by two atmospheric sounding instruments,

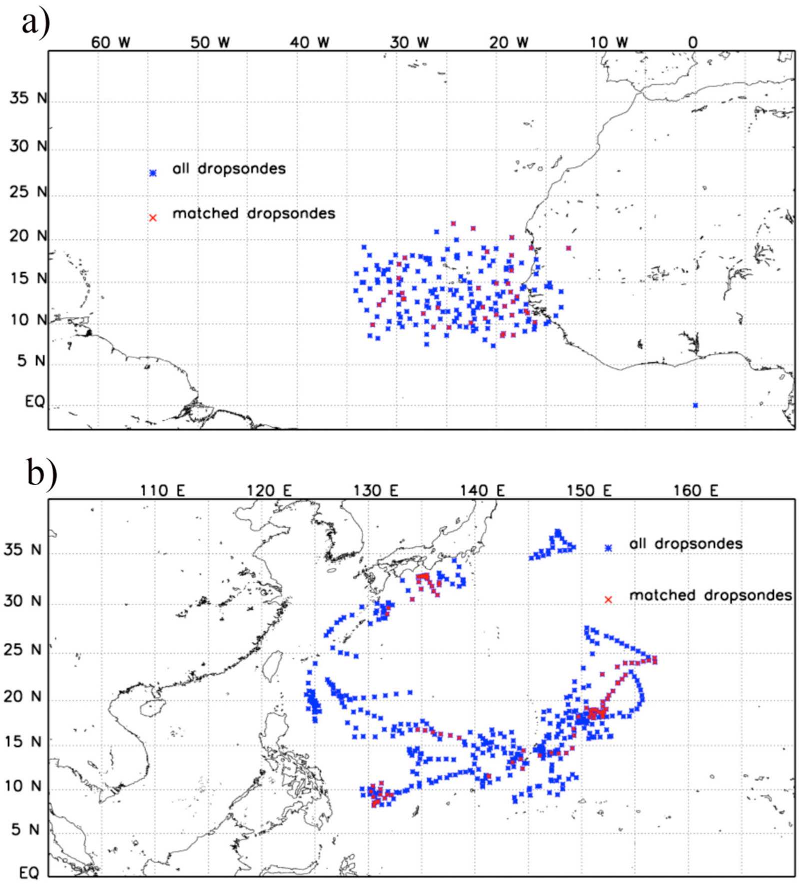


**Figure 1.** The location and data distribution of dropsondes during (a) NAMMA and (b) TPARC field experiments. Red dots that denote these dropsondes are collocated with AIRS data.

the Advanced Microwave Sounding Unit–A (AMSU-A) and the Humidity Sounder for Brazil (HSB). AIRS, AMSU and HSB consist of an innovative atmospheric sounding group of visible, infrared, and microwave sensors. AIRS has 2378 spectral channels including the important temperature sounding region in the 4.2 and 15$\mu$m CO2 bands, water vapor sounding in the 6.3 $\mu$m water vapor band, and ozone sounding in the 9.6 $\mu$m region [*Chahine et al.*, 2006]. The AMSU and HSB instruments are composed of two cross-track scanning multispectral microwave radiometers. A cloud-clearing technique is used to retrieve the temperature and moisture profiles (Level 2 products) [*Susskind et al.*, 2003]. The retrieved AIRS profiles are available in the form of the temperature and water vapor mixing ratio. This study uses the data products from the AIRS retrieval Version 5. In this version, the AIRS Level 2 (version 5.0) retrieved temperature and moisture profiles are available at the 28 standard pressure levels from 1100 to 0.1 hPa. Two characteristic pressure "PBest" and "PGood" are introduced for level 2 temperature quality control. The "PBest" flag indicates that the temperature profile from the top of the atmosphere to this pressure is of best quality. The "PGood" flag indicates that the temperature profile below the level of "PBest" down to this pressure level is of good quality. The retrieved temperature is required to be of good or best quality in this study. The retrieved water vapor profiles are used in this paper when the flag "Qual_H2O" is 1 or 0, meaning that the retrieved moisture is of good or best quality. Note that it is commonly suggested that only these data with quality flag "0" (best) should be used for data assimilation. However, in order to make the use of available data near the tropical cyclones, both data with quality flags " 1" and "0" are also used in this study.

### 2.2. Comparing AIRS Data With Dropsonding Observations From NAMMA and TPRAC Field Experiments Over the Tropical Oceans

[11] The dropsonde soundings were collected from two field campaigns: one is the NAMMA field campaign which was conducted over the Atlantic Ocean during August to September 2006 [*Halverson et al.*, 2007]; the other is the TPARC field campaign which was carried out over West Pacific ocean from August to October 2008 [*Elsberry and Harr*, 2008]. In total, 197 and 475 dropsonde soundings were available from the NAMMA and TPARC field campaigns for this study (Figure 1), respectively. The dropsonde observations include dew point temperature, temperature, relative humidity, wind speed and direction, and geopotential height at pressure levels from surface up to 300 hPa.

[12] AIRS data that were collocated with dropsonde soundings both spatially and temporally were compared with the dropsonding data. Considering the rapid temporal and spatial variations of the atmospheric conditions near the tropical cyclones during their development and movement as well as the sample size of available AIRS data for comparison, the

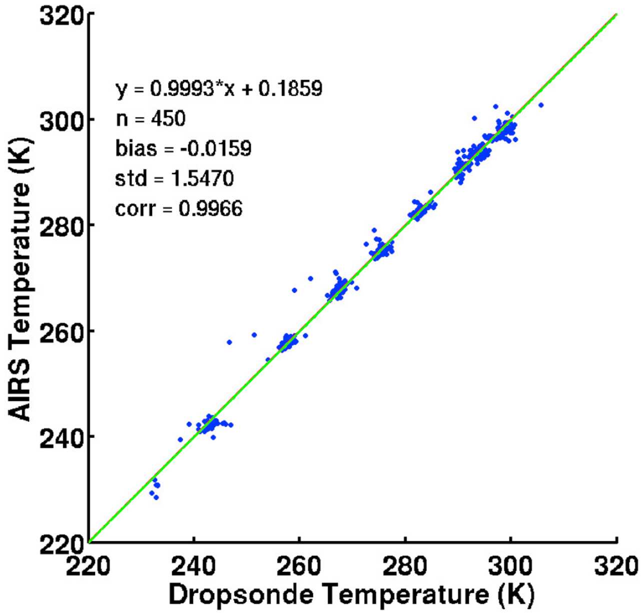


**Figure 2.** Temperature scatterplot of AIRS/Aqua retrievals and NAMMA dropsondes. The red line denotes x = y. The green line shows a linear fit of the data.

maximum time difference is 2 h and the maximum horizontal distance difference between the collocated AIRS profile and the dropsnde sounding is 100 km. Since dropsonde soundings were reported on the high-resolution pressure levels, which were usually from 300 hPa to the surface, the temperature from dropsonde observations was interpolated to the AIRS standard pressure levels from 1000 hPa to 300 hPa, and the dropsonde relative humidity was averaged over the AIRS standard pressure levels. In addition, in this study the drift of the dropsonde position with height was not taken into considerations. Thus, only those data that collocated with a dropsonde pressure level were chosen for comparison. A linear fit was computed for the matched data below 400 hPa both for the NAMMA (2006) and T-PARC (2008) case.

#### 2.2.1. Comparison During NAMMA Over the Eastern Atlantic Ocean

[13] The NAMMA field program was based in the Cape Verde Islands, 350 miles off the coast of Senegal in West Africa. The major research topics of this field program were to examine the formation and evolution of the tropical cyclone over the eastern Atlantic. Thirteen research flights were conducted and 197 dropsonde soundings were collected over the eastern Atlantic (10°N–22°N, 16°W–34°W) between 19 August and 12 September 2006. The quality control of these dropsonde observations has been done by the NAMMA science team (See details in http://namma.msfc.nasa.gov/flighttracks.html).

**Table 1b.** Statistics of the Difference in Temperature Between Dropsondes and AIRS Retrieved Temperature Profiles During NAMMA

| Level (hPa) | Temperature Bias (K) | Temperature RMS (K) | Sample Size |
|---|---|---|---|
| 1000 | −0.63 | 1.52 | 54 |
| 925 | 0.18 | 1.49 | 55 |
| 850 | 0.23 | 1.17 | 57 |
| 700 | −0.20 | 0.83 | 57 |
| 600 | −0.06 | 1.22 | 57 |
| 500 | 0.81 | 1.83 | 58 |
| 400 | 0.34 | 1.93 | 56 |
| 300 | −0.68 | 1.38 | 50 |

[14] A total of 67 matched profiles of these dropsonde soundings were collocated with AIRS data and thus used for comparison (Table 1a). Statistics of the difference in temperature between dropsonde and AIRS retrieved temperature profiles (Table 1b) show good agreement between the two soundings in all pressure levels. The biases are within [−1K,1K] range. The root-mean-square (RMS) errors are less than 2K at all pressure levels. A scatter diagram shows an overall comparison of the temperature profiles with all collocated soundings at all pressure levels (Figure 2). The AIRS temperature retrievals are in very good agreement with the NAMMA soundings, with a correlation coefficient of 0.997 and a RMS difference of 1.55°C. The RMS difference of AIRS temperature (from soundings) is comparable to that found by *Gettelman et al.* [2004], who validated AIRS temperature and relative humidity measurements in the upper troposphere and lower troposphere using aircraft observations.

[15] Compared with the temperature profiles, the statistics of the difference in relative humidity between dropsonde and AIRS retrievals show large discrepancies at all pressure levels (Table 1c). Except the upper levels (between 400 and 300 hPa), in which the bias of AIRS retrieved relative humidity is positive and small, the dry biases are found in all

**Table 1a.** List of Dropsonde Launch Time and Area With The Corresponding AIRS Swathes During NAMMA

| Date | Launch Time (UTC) | Lunch Area | AIRS Swath Time (UTC) |
|---|---|---|---|
| 19 August | 1441–1813 | 7.3°N–14.8°N, 18.4°W–26.2°W | 1441 1447 1623 |
| 20 August | 1259–1834 | 8.2°N–13.8°N, 28.1°W–32.6°W | 1347 1353 1523 1529 1535 |
| 23 August | 1235–1621 | 15.1°N–19.1°N, 26.8°W–34.0°W | 1417 1423 1559 1605 |
| 25 August | 1325–1921 | 9.0°N–20.0°N, 16.1°W–20.9°W | 1405 1411 1547 1553 |
| 26 August | 1313–1746 | 11.1°N–21.9°N, 19.6°W–30.0°W | 1317 1447 1453 |
| 30 August | 1336–1804 | 10.1°N–20.0°N, 21.1°W–24.2°W | 1423 1429 1605 1611 |
| 01 September | 1331–1814 | 9.3°N–17.7°N, 13.4°W–22.7°W | 1411 1417 1553 1559 |
| 03 September | 1217–1755 | 11.4°N–18.3°N, 19.0°W–27.9°W | 1359 1405 1541 1547 |
| 04 September | 1333–1745 | 10.2°N–18.0°N, 26.4°W–34.1°W | 1311 1441 1447 1623 |
| 05 September | 1228–1323 | 18.9°N–19.0°N, 12.7°W–20.0°W | 1347 1353 |
| 08 September | 1337–1830 | 8.6°N–17.5°N, 14.6°W–22.3°W | 1417 1423 1559 1605 |
| 09 September | 1349–1559 | 9.5°N–14.2°N, 22.3°W–27.3°W | 1329 1459 1505 |
| 12 September | 1220–1557 | 10.5°N–15.6°N, 20.0°W–26.0°W | 1353 1359 |

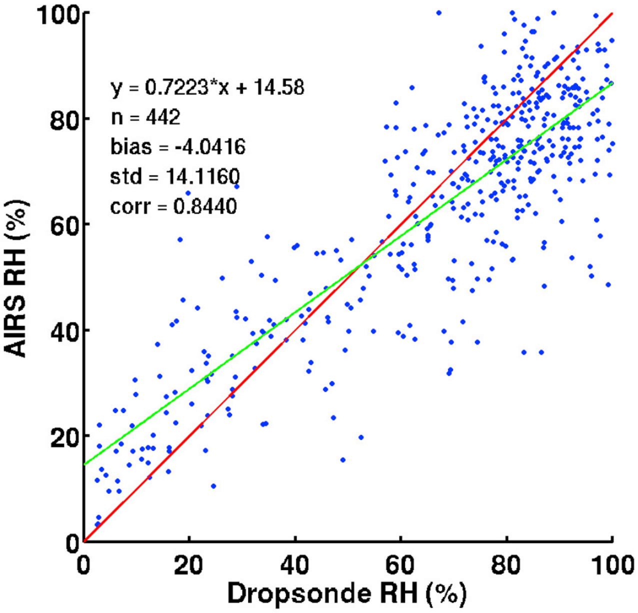


**Figure 3.** Relative humidity scatterplot of AIRS/Aqua retrievals and NAMMA dropsondes. The red line denotes x = y. The green line shows a linear fit of the data.

levels below 400 hPa. The RMS differences of relative humidity between two soundings near or exceed 10% at all levels. Overall, a wide scatter for relative humidity with a negative bias of −4.04% is found over the data at all pressure levels (Figure 3). The correlation coefficient between the AIRS and NAMMA relative humidity is about 84% with a RMS difference of 14%.

#### 2.2.2. Comparison During TPARC Over the Western Pacific Ocean

[16] During the months of August and September 2008, a multinational field campaign commenced in the Western Pacific tropical basin. Under the umbrella of the THORPEX Pacific Asian Regional Campaign (T-PARC), the Tropical Cyclone Structure Program (TCS-08, sponsored by U.S. Office of Naval Research) investigated the mechanisms and predictability of tropical formation, development and extatropical transition (for details see *Elsberry and Harr* [2008]). During the TPARC field experiments, a total of 24 aircraft missions with over 500 flight hours were conducted. The aircraft operations include the U.S. Naval Research Laboratory's P-3 (NRL P-3; operated during 10 August to 3 October), the U.S. Air Force's WC-130J (UAF 130C; operated during 1 August to 30 September) based in Guam and operated over the North West Pacific Ocean, the German DLR Falcon based in Japan (operated during 25 August to 1 October), and the Taiwan DOTSTAR aircraft (only operated when major typhoons were approaching Taiwan). Since we would like to emphasize the North Western Pacific only for uses of comparison in this study, the dropsonde data collected by NRL P-3 and UAF 130C are used in the analysis. A total of 475 dropsonde soundings are available after a quality control procedure by the National Center for Atmospheric Research (NCAR, see detailed document about the quality control on web site http://data.eol.ucar.edu/).

[17] In all, 114 matched profiles between aircraft dropsondes and AIRS retrieved soundings were found (Table 2a). Statistics of the difference of temperature between dropsonde and AIRS retrieved temperature profiles (Table 2b) show good agreement between two soundings at all pressure levels. The biases are within [−1.5K,1.5K] range. The RMS errors are less than 2K at all pressure levels. An overall comparison of the temperature profiles is also shown by a scattering diagram with all collocated soundings at all pressure levels (Figure 4). The AIRS temperature retrievals are in very good agreement with the TPRAC sounding with a correlation coefficient of 0.991 and a RMS difference of 1.5°C. The results indicate that the quality of temperature retrievals is similar in both the Atlantic and Western Pacific.

[18] However, the statistics of the difference of relative humidity between dropsonde and AIRS data show large discrepancies at all pressure levels (Table 2c). Except the level between 925 and 850 hPa, which presents a wet bias of AIRS retrieved relative humidity of about 4.42%, the dry biases are found at other levels with various degrees. The RMS differences of relative humidity between two soundings show about 10% discrepancies in all levels below 600 hPa. Overall, a large scatter for relative humidity with a bias of −5.2% is found over the data at all pressure levels (Figure 5). The correlation coefficient between the AIRS and TPARC dropsondes relative humidity is about 54% with a RMS difference of 12%. Overall, the AIRS moisture retrievals proved to be too dry, which is consistent with what has been found in Atlantic Ocean. The correlations between the AIRS retrieved relative humidity and TPARC dropsonde sounding is somewhat lower compared with the correlations between the AIRS retrievals and NAMMA dropsondes (54% versus 84%).

## 3. Impact of AIRS Retrieved Temperature and Moisture Profiles on Tropical Cyclone Forecasts

[19] The above results show that the biases existed in AIRS retrievals. In this section, we examine the potential impacts of the data and the impact of bias correction on the numerical simulations of tropical cyclones. Two cases were arbitrarily chosen based on the availability of the AIRS retrieved profiles: one is Tropical Storm Debby (2006) over the eastern Atlantic Ocean during its formation; the other one is Typhoon Jangmi (2008) over the western Pacific Ocean during its mature phase.

### 3.1. Brief Description of WRF Model and Its 3DAVR System

[20] The WRF model is a recently developed mesoscale numerical weather prediction system. It is designed to serve both operational forecasting and atmospheric research

**Table 1c.** Statistics of the Difference in Relative Humidity Between Dropsondes and AIRS Retrieved Moisture Profiles During NAMMA

| Layer (hPa) | RH Bias (%) | RH RMS (%) | Sample Size |
|---|---|---|---|
| 1000–925 | −6.22 | 9.35 | 65 |
| 925–850 | −1.54 | 10.64 | 64 |
| 850–700 | −3.34 | 12.94 | 65 |
| 700–600 | −3.95 | 14.71 | 61 |
| 600–500 | −10.02 | 16.11 | 64 |
| 500–400 | −5.18 | 15.59 | 60 |
| 400–300 | 0.63 | 12.93 | 55 |

**Table 2a.** List of Dropsonde Launch Time and Area With the Corresponding AIRS Swathes During T-PARC

| Date | Launch Time (UTC) | Lunch Area | AIRS Swath Time (UTC) |
|---|---|---|---|
| 12 August | 0516–0517 | 11.5°N–12.5°N, 140.5°E–141.5°E | 0423–0435 0605–0617 |
| 16 August | 0001–0358 | 12.0°N–17.0°N, 141.0°E–46.0 °E | 0223 0229 0235 0359 0405 0411 |
| 17 August | 0007–0248 | 15.0°N–17.0°N, 135.0°E–142.0°E | 0305 0311 0317 |
| 18 August | 0000–0346 | 15.5°N–18.0°N, 131.0°E–138.0°E | 0211 0217 0223 0347 0353 0359 |
| 28 August | 0041–0545 | 14.0°N–19.0°N, °145.0E–153.0°E | 0247 0253 0259 0423 0429 0435 0605 0611 0617 |
| 29 August | 0020–0410 | 13.0°N–20.0 °N, 150.0°E–156.0°E | 0159 0205 0329 0335 0341 0511 |
| 01 September | 1930–2351 | 11.5°N–16.0°N, 140.0°E–144.0°E | 1929 1935 |
| 08 September | 0045–0648 | 17.0°N–28.0°N, 147.0°E–157.0°E | 0229 0235 0241 0405 0411 0417 0547 0553 0559 |
| 09 September | 0220–0654 | 13.0°N–22.0°N, 146.0°E–151.0°E | 0311 0317 0323 0447 0453 0459 0629 0635 0641 |
| 11 September | 0004–0210 | 20.0°N–23.0°N, 126.0°E–128.0°E | 0259 0305 0311 |
| 13 September | 2023–2349 | 13.0°N–19.0°N, 146.0°E–153.0°E | 1953 |
| 14 September | 0003–0149 | 14.0°N–19.0°N, 146.2°E–151.0°E | 0159 0205 2035 |
| 16 September | 2108–2145 | 141.5°N–144.2°N, 14.0°E–15.5°E | 2023 |
| 17 September | 0040–0312 | 24.5°N–30.5°N, 126.0°E–132.0°E | 0223 0229 0235 0359 0405 0411 |
| 18 September | 0109–0403 | 28.5°N–30.0°N, 129.2°E–132.5°E | 0305 0311 0317 0441 0447 0453 |
| 19 September | 0100–0524 | 30.5°N–33.5°N, 133.1°E–138.9°E | 0211 0217 0223 0347 0353 0359 0529 0535 0541 |
| 20 September | 0616–0820 | 34.5°N–37.5°N, 145.2°E–149.5°E | 0611 0617 0623 |
| 22 September | 0004–0432 | 17.5°N–21.9°N, 124.1°E–125.5°E | 0241 0247 0253 0417 0423 0429 |
| 23 September | 0418–0606 | 10.3°N–13.0°N, 139.5°E–141.5°E | 0323 0329 0335 0505 0511 0517 0641 0647 0653 |
| 27 September | 0005–0225 | 18.0°N–20.9°N, 127.2°E–131.2°E | 0259 0305 0311 0435 0441 0447 |
| 03 October | 0005–0340 | 8.5°N–14.6°N, 137.5°E–149.4°E | 0223 0229 0235 0359 0405 |
| 04 October | 0009–0700 | 8.1°N–11.5°N, 129.3°E–136.7°E | 0305 0311 0317 0441 0447 0453 0623 0629 0635 |

needs. The WRF model features multiple dynamic cores. This study employs the advanced research WRF (ARW) core developed by NCAR. The ARW carries multiple physical options for cumulus, microphysical, PBL and radiative physical processes. Details of the model are provided by *Skamarock et al.* [2008]. Version 3 of the ARW model is used for the experiments in this study.

[21] Along with the ARW, a three-dimensional variational data assimilation (3DVAR) system was developed [*Barker et al.*, 2004a, 2004b] to fulfill the data assimilation needs for model initialization. The 3DVAR system provides an analysis $x^a$ via the minimization of a prescribed cost function $J(x)$:

$$J(x) = J^b + J^o = \frac{1}{2}\left(x - x^b\right)^T B^{-1}\left(x - x^b\right) + \frac{1}{2}\sum_{i=0}^{n}\left(y - y_i^0\right)^T O_i^{-1}\left(y - y_i^0\right) \qquad (1)$$

In (1), the analysis $x = x^a$ represents a posteriori maximum likelihood (minimum variance) estimate of the true state of the atmosphere given two sources of data: the background (previous forecast) $x^b$ and observations $y^o$ [*Lorenc*, 1986]. The analysis fit to these data is weighted by estimates of their errors: ***B*** and ***O*** are the background and observational error covariance matrices, respectively. Here $y = H(x)$ and $H$ is a linear or nonlinear operator used to transform the grid point analysis x to observational space and type. In equation (1), $i$ denotes each type of observational data and $n$ represents the total number of data types. For the 3DVAR experiment, the background error covariance matrix ***B*** was estimated using the so-called NMC [National Meteorological Center, now known as NCEP] method [*Parrish and Derber*, 1992; *Barker et al.*, 2004a]. The observational error covariance matrices, ***O***, were treated as diagonal matrices with statistically determined variances of the observational data.

**Table 2b.** Statistics of the Difference in Temperature Between AIRS and Dropsondes Retrieved Temperature Profiles During T-PARC

| Level (hPa) | Temperature Bias (K) | Temperature RMS (K) | Sample Size |
|---|---|---|---|
| 1000 | −1.04 | 1.72 | 33 |
| 925 | −1.36 | 1.47 | 33 |
| 850 | −0.94 | 1.52 | 33 |
| 700 | −0.47 | 0.90 | 24 |
| 600 | 0.31 | 0.89 | 22 |
| 500 | 1.16 | 0.71 | 9 |
| 400 | −0.64 | 0.56 | 7 |

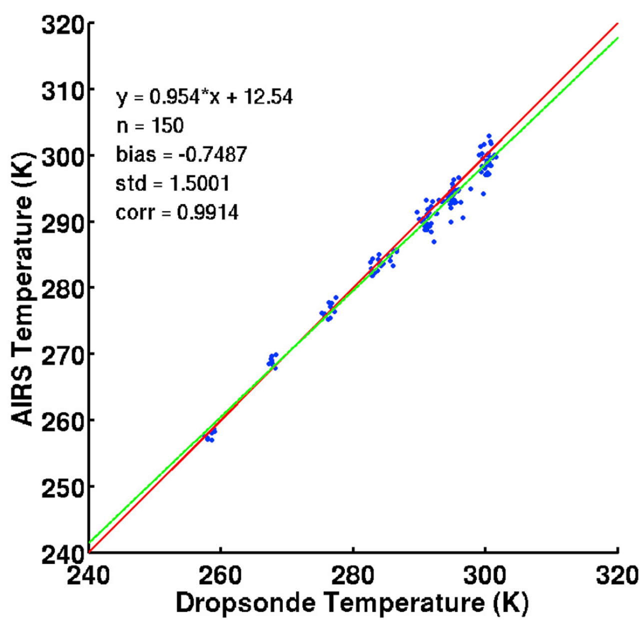


**Figure 4.** Same as Figure 2, except for the temperature scatterplot of AIRS/Aqua retrievals and TPARC dropsondes.

**Table 2c.** Statistics of the Difference in Relative Humidity Between AIRS and Dropsondes Retrieved Moisture Profiles During T-PARC

| Layer (hPa) | RH Bias (%) | RH RMS (%) | Sample Size |
|---|---|---|---|
| 1000–925 | −2.27 | 13.34 | 69 |
| 925–850 | 4.42 | 11.29 | 70 |
| 850–700 | −8.39 | 9.36 | 58 |
| 700–600 | −11.76 | 12.51 | 35 |
| 600–500 | −5.29 | 6.34 | 13 |
| 500–400 | −0.40 | 7.07 | 10 |

### 3.2. Numerical Experiment for Debby

[22] Tropical Storm Debby (2006) was developed from an African easterly wave (AEW) over land. After moving offshore, circulation developed quickly. Debby was classified as a tropical depression at 1800 UTC 21 August 2006. It evolved into a tropical storm at 0000 UTC 23 August 2006. Due to dry and stable air, along with marginal sea surface temperatures (SST), Debby never intensified into a hurricane. Shear associated with an approaching upper level trough eventually caused the cyclone to dissipate.

[23] Since it is commonly recognized that the Sahel air layer (SAL) plays an important role in tropical storm formation, the objective of the numerical simulation of Debby is to examine the impact of AIRS data on the numerical simulation of Debby's development and formation. Therefore, we chose 1200 UTC 21 August 2006 as initial conditions. For the experiments, the data from the National Centers for Environmental Prediction (NCEP) global final analysis (FNL) on a 1.0 × 1.0 degree grid were used to provide boundary conditions for the numerical simulations. Instead of directly using the NCEP FNL analysis for the first guess in the 3DVAR experiments, a WRF simulation, initialized by the WRF standard initialization process package using the NCEP FNL analysis, was first integrated 6 h to provide a first guess field for the 3DVAR data assimilation. The control experiment (CNTL) assimilates available conventional data but no AIRS data are incorporated.

[24] For the numerical simulation, model physics options include the *Grell and Devenyi* [2002] cumulus parameterization, Purdue Lin microphysics scheme, the Mellor-Yamada-Janjic (MYJ) planetary boundary layer parameterization (see detailed description of these schemes by *Skamarock et al.* [2008]), and the Rapid Radiative Transfer Model (RRTM) [*Mlawer et al.*, 1997] longwave and Dudhia shortwave atmospheric radiation [*Dudhia*, 1989] schemes. A two-way interactive, two-level nested grid technique is employed to achieve the multiscale forecast. The outer domain resolution has 27 km grid spacing and the inner domain resolution is 9 km, with grid dimension 307 × 187 and 385 × 361 for two domains, respectively. The model vertical structure is composed of 31 $\sigma$ levels with the top of the model set at 50 hPa, where $\sigma = (p_h - p_{ht})/(p_{hs} - p_{ht})$ while $p_h$ is the hydrostatic component of the pressure, and $p_{hs}$ and $p_{ht}$ refer to values of the pressure along the surface and top boundaries, respectively. The $\sigma$ levels are placed close together in the low levels (below 500 hPa) and are relatively coarsely spaced above.

[25] Considering the data availability, the 3DVAR data assimilation experiments were performed for the period of 1200 UTC 21 August 2006 to 1200 UTC 22 August 2006. There were total of four AIRS satellite swathes that passed over the model domain (Figure 6). Four data assimilation cycles were performed during the period. The forecast was then conducted during the period of 1200 UTC 22 August 2006 to 1200 UTC 23 August 2006, when Debby became a tropical storm. In order to examine the impact of the bias correction on the forecast of Debby's development, six different experiments were performed: (1) control experiment without assimilation of AIRS data, as mentioned above; (2) assimilation of moisture profiles without bias correction; (3) assimilation of moisture profiles with bias correction; (4) assimilation of temperature profiles without bias correction; (5) assimilation of temperature profiles with bias correction; and (6) assimilation of both moisture profiles and temperature profiles with bias correction. In all experiments, available conventional data were assimilated. There were no dropsonde data available in the model domain during the assimilation period. The biases of the temperature and moisture profiles follow the numbers listed in the Tables 1b and 1c for the different pressure levels. Since there is no bias information available for these AIRS retrieved temperature and moisture profiles above 300 hPa, only these data at and below 300hPa are assimilated.

[26] Figure 7 shows the forecasted sea level pressure, surface wind and 3 h accumulated precipitation of Debby at 1200 UTC 23 August 2006. According to National Hurricane Center (NHC), at the time Debby should be a tropical storm with a maximum wind speed of 23 m s$^{-1}$ and organized convective rainfalls. Figure 8 presents the corresponded 3 hourly rainfall rate from NASA Tropical Rainfall Measuring Mission (TRMM) real-time rainfall product [*Huffman et al.*, 2007]. However, in the control experiment (Figure 7a), the forecast produces a tropical depression and the location is northeast of the actual storm location. The intensity of the depression is also too weak when compared with the observed intensity.

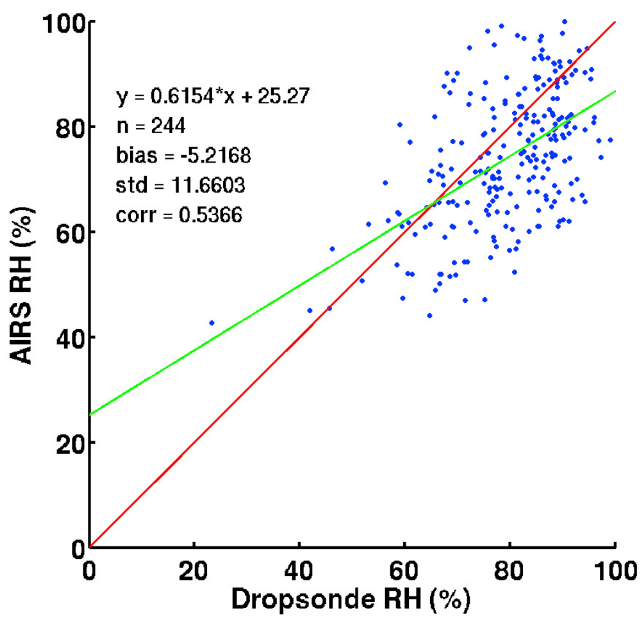


**Figure 5.** Same as Figure 3, except for the relative humidity scatterplot of AIRS/Aqua retrievals and TPARC dropsondes.

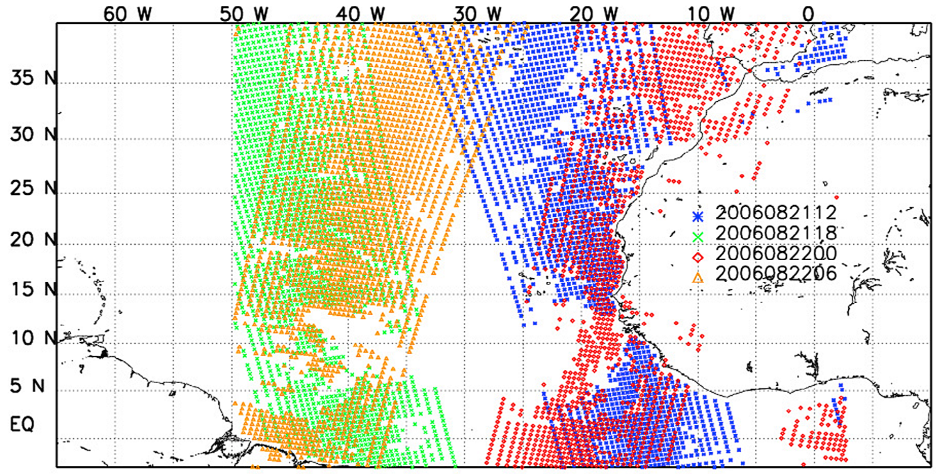


**Figure 6.** The location and data distribution of AIRS data swathes between 1200 UTC 21 August 2006 to 0600 UTC 22 August 2006.

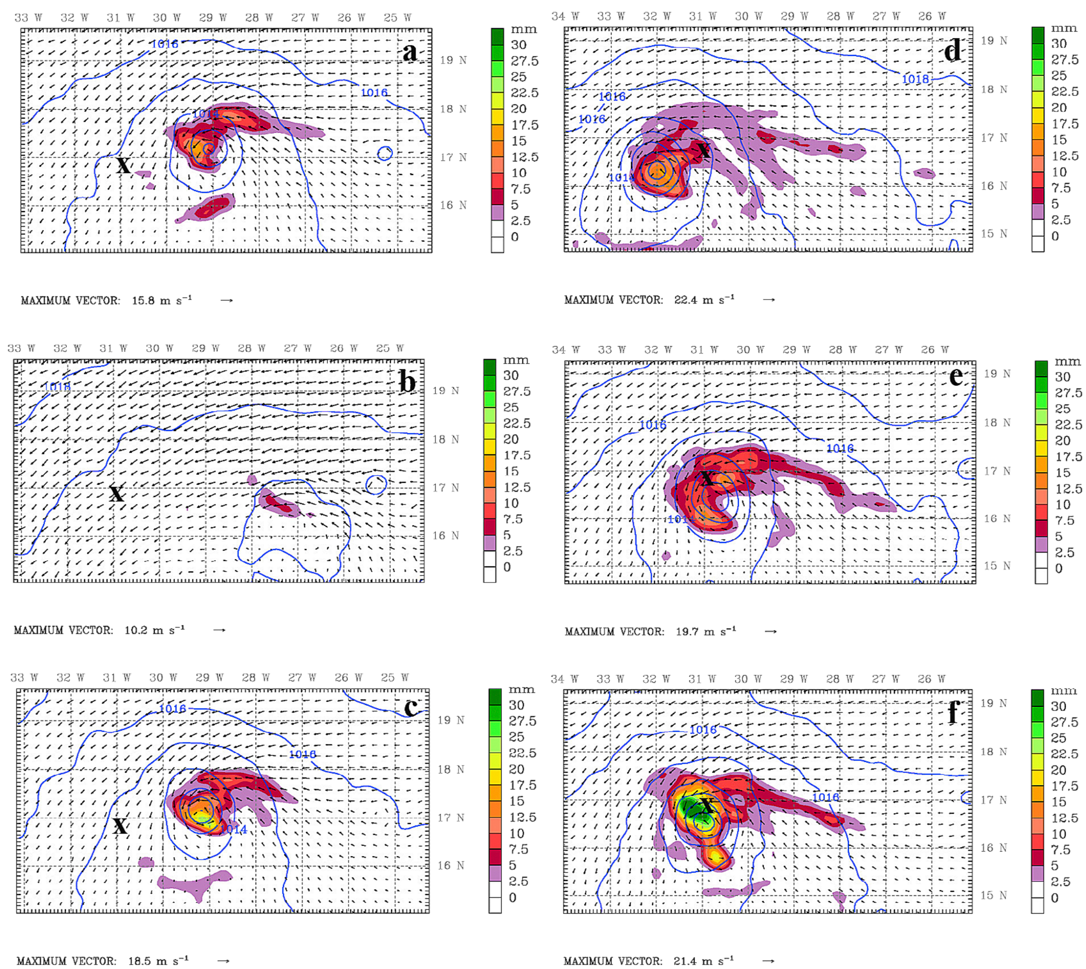


**Figure 7.** Numerical simulations of sea level pressure (line contour, interval 1 hPa), wind vector at lowest model sigma level, and 3 h accumulated precipitation (shaded contour, unit mm) at 1200 UTC 23 August 2006 from different experiments: (a) control, without assimilation of AIRS data; (b) assimilation of AIRS moisture profiles without bias correction; (c) assimilation of AIRS moisture profiles with bias correction; (d) assimilation of AIRS temperature profiles without bias correction; (e) assimilation of AIRS temperature profiles with bias correction; (f) assimilation of both temperature and moisture profiles with bias corrections. "X" denotes the best track position of Debby.

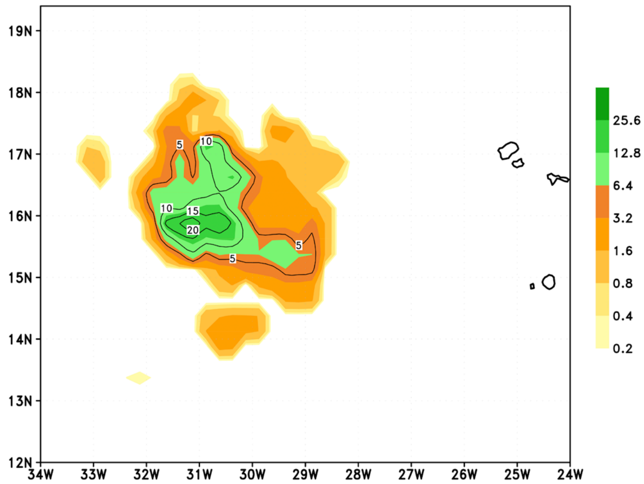


**Figure 8.** The 3 h accumulated rainfall (mm) from the Tropical Rainfall Measuring Mission (TRMM) 3B42 products at 1200 UTC 23 August 2006.

[27] We first examine the impact of the quality of moisture data on the numerical simulation of Debby. Without bias correction, the assimilation of the moisture data led to a forecast in which Debby was dissipated. The tropical depression and its associated circulation disappeared over the ocean (Figure 7b). Then, a bias correction was applied to moisture data before assimilating them into the model. Figure 7c shows that the model generates a fairly reasonably forecast of the tropical storm after assimilating the corrected moisture data into the ARW model. Both storm development and the intensity of the convection agree with the NHC best track data and TRMM rainfall observations (Figure 8).

[28] The assimilation of the temperature profiles resulted in a significant influence on the storm track forecast, while it also improved the convective structure of the storm (Figures 7d and 7e). Without bias correction, the assimilation of the temperature data deflects the position of Debby further west in the forecasts. With bias correction, the assimilation of the temperature data resulted in an accurate track forecast for Debby.

[29] With the assimilation of both bias-corrected temperature and moisture profiles, the numerical simulation produced a tropical storm Debby with reasonable structure, intensity and position. The simulated 3 hourly rainfall structure and intensity matches the TRMM observations at the time (Figure 8).

[30] The negative impact of moisture data assimilation without bias correction can be attributed to the dry bias of the data. Figure 9 shows the analysis increments at the end of the last data assimilation cycle (1200 UTC 22 August 2006) at different pressure levels (850 hPa and 700 hPa) in the moisture field for Experiment 2 and 3 (assimilation of moisture profiles without and with the bias correction). A noticeably drier air ingest from the environment was found in all levels in the forecast experiment without the bias correction. With the bias correction, the dry analysis increments were eliminated in all levels. The fact that the temperature assimilation results in a significant impact on track forecasts is mainly due to the large response from the wind field.

### 3.3. Numerical Experiment for Jangmi

[31] Jangmi originated as an area of intense convection east of Guam on 16 September 2008. Intermittent and scattered convection continued through 23 September. The Joint Typhoon Warning Center (JTWC) designated the system a tropical depression at 1800 UTC, followed by tropical storm status at 0000 UTC 24 September. At 0600 UTC 25 September, the cyclone reached typhoon status. With gradual strengthening on 26 September, forward motion slowed. Rapid intensification into super typhoon status occurred on 27 September, but it then weakened prior to crossing Taiwan on 28 September. Since Jangmi was a notable super Typhoon during the 2008 typhoon season, we chose to examine the impact of AIRS data on the numerical simulation of Typhoon Jangmi right at the time when it reaches typhoon intensity. AIRS retrievals are assimilated at 0600 UTC 25 September 2008 (data swathes are shown in Figure 10) and numerical simulations were conducted during the period of 0600 UTC 25 to 0600 UTC 27 September 2008.

[32] Similar to the numerical experiments for Debby as mentioned above, a two-way interactive, two-level nested grid technique is employed to achieve the multiscale forecast. The outer domain resolution has a 27 km grid spacing and the inner domain resolution is 9 km. The model vertical structure is composed of 31 $\sigma$ levels with the top of the model set at 50 hPa. Model physics options include the Betts-Miller-Janjic cumulus parameterization, WSM six-class graupel microphysics scheme [*Hong and Lim*, 2006], the Yonsei University (YSU) planetary boundary layer parameterization, and the Rapid Radiative Transfer Model (RRTM) [*Mlawer et al.*, 1997] longwave and Dudhia shortwave atmospheric radiation [*Dudhia*, 1989].

[33] Six different experiments are conducted for Jangmi: (1) control experiment without AIRS data assimilation; (2) assimilation of moisture profiles with bias correction; (3) assimilation of moisture profiles without bias correction; (4) assimilation of temperature profiles with bias correction; (5) assimilation of temperature profiles without bias correction; and (6) assimilation of both moisture profiles and temperature profiles with bias correction. In all experiments, available conventional observations and dropsonding profiles (only four profiles fell into the model domain) are assimilated. The bias corrections for the temperature and moisture profiles follow the numbers listed in the Table 2b.

[34] Numerical simulation results showed positive impact of the AIRS data assimilation on the track forecasting of Jangmi. Figure 11 show the track and track errors from different experiments. It is obvious that the forecast of Jangmi's track is sensitive to the assimilation of the AIRS retrieved profiles. Specifically, the assimilation of temperature profiles has significant impact on Jangmi's track forecasting. With bias correction, assimilating AIRS retrieved temperature profiles resulted in a better track forecast, compared with the experiment without bias correction for the AIRS retrieved temperature profiles. The track errors are very similar in both experiments with and without bias correction for moisture profiles, mainly because the overall track improvement from moisture data assimilation is relatively small. Assimilation of both temperature and moisture profiles resulted in the largest improvement in the track forecast.

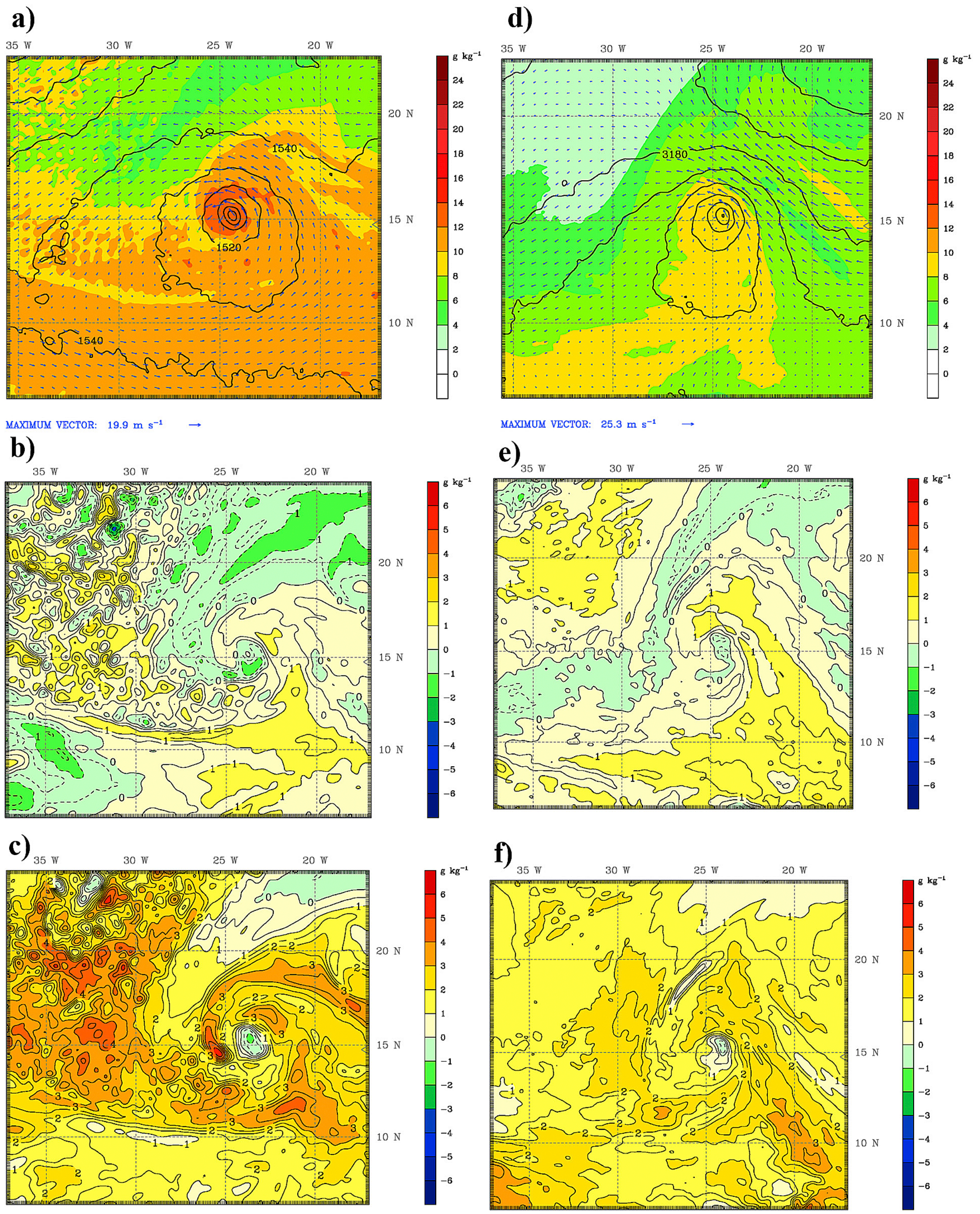


**Figure 9.** Numerical simulations of vector wind, geopotential height (contours in Figures 9a and 9d) and water vapor mixing ratio (shaded contours in Figures 9a and 9d), analysis increments in water vapor mixing ration from experiments assimilating AIRS moisture profiles without (Figures 9b and 9e) and with (Figures 9c and 9f) bias correction from (a–c) 850 and (d–f) 700 pressure levels at 1200 UTC 22 August 2006.

[35] For this particular case, the improvement in intensity is very marginal from the assimilation of AIRS temperature and moisture profiles., This can be attributed to the fact that Jangmi has been a matured typhoon during the simulation period and most of the AIRS profiles are distributed in the typhoon environment instead of its inner core area. *Pu et al.* [2009] found that the accurate representation of inner core structures has more impact on intensity forecasts of a matured tropical cyclone.

## 4. Concluding Remarks

[36] Tropical cyclones usually develop over the oceans where conventional observations are very sparse. Numerical

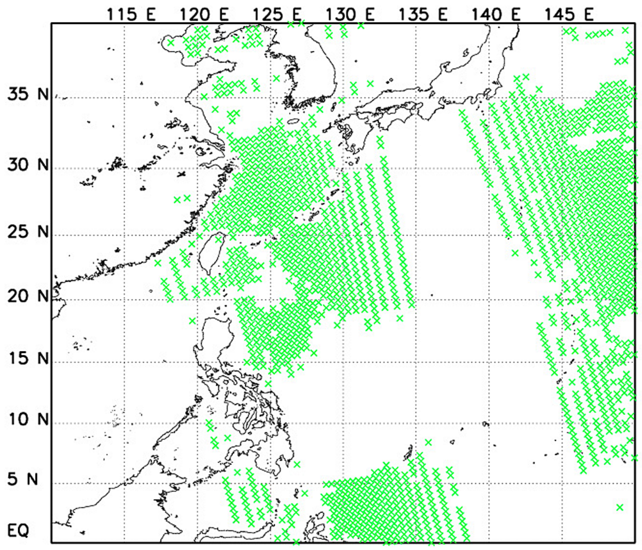


**Figure 10.** The location and data distribution of AIRS data swathes at 0600 UTC 25 September 2008.

simulations and forecasts of tropical cyclones are sensitive to the accuracy of initial conditions. Satellite data, such as the AIRS retrieved temperature and moisture profiles provide significant data sources for improving the forecasts of tropical cyclone genesis, development and intensification. However, the accuracy of initial conditions depends not only on the data assimilation technique itself, but also on the quality of the data.

[37] In this study, the quality of the retrieved temperature and moisture profiles acquired from AIRS, aboard the NASA Aqua spacecraft, was evaluated by comparing the data with dropsonde observations obtained from NASA African Monsoon Multidisciplinary Analyses (NAMMA) and international THORPEX Pacific Asian Regional Campaign (T-PARC) field programs. It is found that

[38] 1. The AIRS retrieved temperature profiles, although with small biases, are in good agreement with dropsonde observations near the tropical cyclone environment. However, the AIRS retrieved moisture profiles show a larger bias (mostly dry bias) compared with the dropsondes over the tropical oceans where tropical cyclones developed.

[39] 2. Results from data assimilation experiments show that assimilation of the AIRS retrieved temperature and

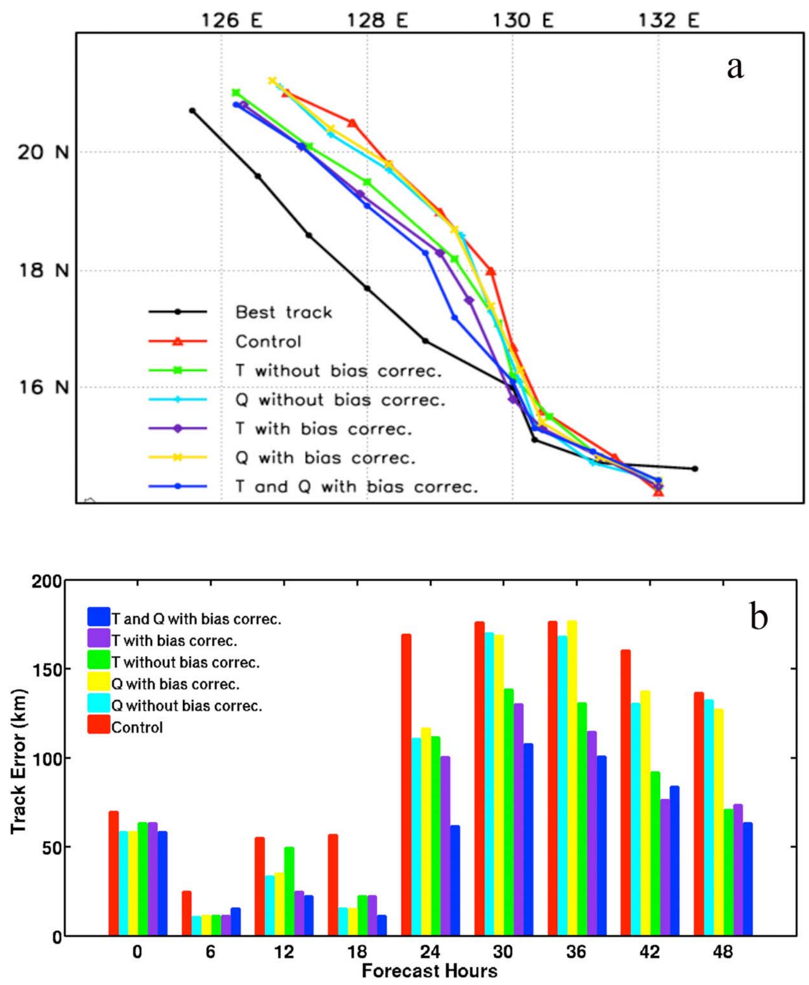


**Figure 11.** (a) Jangmi's track and (b) track errors during 0600 UTC 25 September 2008 to 0600 UTC 27 September 2008 from different experiments and compared with the JTWC best track data.

moisture profiles have a significant impact on the numerical simulations of tropical cyclones, however, the overall impacts of the data on numerical simulations of tropical cyclones are very sensitive to the bias corrections of the data. Specifically, the dry biases of moisture profiles cause the decay of the Tropical Storm Debby (2006) in the numerical simulations. Even small biases in temperature profiles would result in errors in the track forecasting. Only with bias correction, the simulation results in a reasonable portrayal of storm development.

[40] 3. Compared with the moisture profiles, temperature profiles have a larger impact on typhoon track forecasting. Assimilation of the temperature data resulted in significant improvements in the track forecasts for both Tropic Storm Debby (2006) and Typhoon Jangmi (2008).

[41] The sensitivity of numerical simulations of Tropical Storm Debby to moisture data implies that the moisture field plays an important role in the prediction of tropical cyclone formation over the tropical oceans. Therefore, accurate moisture retrievals should be very important in numerical forecasts of tropical cyclone formation. Further studies should emphasize on examining the impact of moisture data on numerical predictions of the tropical cyclone genesis and evolution. In addition, more robust bias correction schemes need to be developed, subject to more in situ data available in the future.

[42] Despite the impact of the data and the importance of the bias correction shown in this paper, it should be noted that the data biases are different in two different basins. Larger biases and lower correlations in the moisture data are found over the Western Pacific Ocean than over the Atlantic Ocean. Further study is needed to carefully compare the data quality over two ocean basins. Compared with the areas over the Atlantic Ocean, the Pacific Ocean is vast and largely void of observations; more data will thus be needed in order to calibrate and validate the data quality in the area.

[43] In addition, it should be also noted that in this study we validated the AIRS retrieved temperature and moisture profiles near the tropical cyclone environment, where the sky conditions with cloud activities because many NAMMA and T-PARC dropsondes were released in the cloud clusters or in the circulation of named tropical cyclones. It is well known that cloud activities can degrade the accuracy of the AIRS retrievals [*Divakarla et al.*, 2006; *Tobin et al.*, 2006]. Fortunately, although the large discrepancies are found between AIRS retrieved moisture profiles and dropsondes, the RMS errors for the cases in this study are still close to the design expectation for clear sky conditions [*Fetzer et al.*, 2003].

[44] Furthermore, the dry biases of moisture profiles found in this paper were not explicitly addressed in previous evaluations from other studies [e.g., *Gettelman et al.*, 2004; *Divakarla et al.*, 2006] although these studies also showed the discrepancies between AIRS retrieved water vapor and soundings in a range of up to 10 to 15%. The different conclusion from this study can be attributed to the cloud sky conditions used in the comparison, while most of previous evaluations were conducted under the clear-sky conditions.

[45] As this manuscript was nearly complete, we realized that *Wu* [2009] had conducted a study to compare the NAMMA dropsonding data with AIRS retrieved temperature and moisture profiles. While both this study and *Wu* [2009] found that uncertainty of AIRS retrieved temperature and moisture profiles is within design expectations, the detailed comparison methods (in terms of data quality flags used, time window to match the AIRS data with dropsondes) are different.

[46] **Acknowledgments.** The authors would like to thank the NASA AIRS science team, NAMMA science team and Office of Naval Research (ONR) TCS-08 science team, and NCAR EOL data management system (sponsored by NSF). Some useful discussion with Eric Fetzer and Bjorn Lambrigtsen at JPL/NASA are greatly appreciated. Review comments from three anonymous reviewers were very helpful to improve the manuscript. The computer time for this study was provided by NASA High-End Computing System and the Center for High Performance Computing (CHPC) at the University of Utah. This study is supported by ONR grant N000140810308 and NASA grant NNX08AD32G.

## References

Atlas, R. (2005), The impact of AIRS data on weather prediction, in *Algorithms and Technologies for Multispectral, Hyperspectral, and Ultraspectral Imagery XI*, edited by S. Shen and P. Lewis, *Proc. SPIE*, 5806, 599–606.

Aumann, H. H., et al. (2003), AIRS/AMSU/HSB on the Aqua mission: Design, science objectives, data products, and processing system, *IEEE Trans. Geosci. Remote Sens.*, *41*, 253–264, doi:10.1109/TGRS.2002.808356.

Barker, D. M., W. Huang, Y. R. Guo, and Q. N. Xiao (2004a), A three-dimensional (3DVAR) data assimilation system for use with MM5: Implementation and initial results, *Mon. Weather Rev.*, *132*, 897–914, doi:10.1175/1520-0493(2004)132<0897:ATVDAS>2.0.CO;2.

Barker, D. M., M.-S. Lee, Y.-R. Guo, W. Huang, Q.-N. Xiao, and R. Rizvi (2004b), WRF variational data assimilation development at NCAR, paper presented at WRF/MM5 Users' Workshop, Boulder, Colo., 22–25 June.

Chahine, M. T., et al. (2006), Improving weather forecasting and providing new data on greenhouse gases, *Bull. Am. Meteorol. Soc.*, *87*, 911–926, doi:10.1175/BAMS-87-7-911.

Chen, S. H. (2007), The Impact of assimilating SSM/I and QuikSCAT satellite winds on Hurricane Isidore simulation, *Mon. Weather Rev.*, *135*, 549–566, doi:10.1175/MWR3283.1.

Derber, J. C., and W.-S. Wu (1998), The use of TOVS cloud-cleared radiances in the NCEP SSI analysis system, *Mon. Weather Rev.*, *126*, 2287–2299, doi:10.1175/1520-0493(1998)126<2287:TUOTCC>2.0.CO;2.

Divakarla, M. G., C. D. Barnet, M. D. Goldberg, L. M. McMillin, E. Maddy, W. Wolf, L. Zhou, and X. Liu (2006), Validation of Atmospheric Infrared Sounder temperature and water vapor retrievals with matched radiosonde measurements and forecasts, *J. Geophys. Res.*, *111*, D09S15, doi:10.1029/2005JD006116.

Dudhia, J. (1989), Numerical study of convection observed during the winter monsoon experiment using a mesoscale two-dimensional model, *J. Atmos. Sci.*, *46*, 3077–3107, doi:10.1175/1520-0469(1989)046<3077:NSOCOD>2.0.CO;2.

Elsberry, R. L., and P. A. Harr (2008), Tropical cyclone structure (TCS0field 8) experiment science basis, observational platforms, and strategy, *Asia Pac. J. Atmos. Sci.*, *44*, 1–23.

Errico, R. M., G. Ohring, F. Weng, P. Bauer, B. Ferrier, J.-F. Mahfouf, and J. Turk (2007), Assimilation of satellite cloud and precipitation observations in numerical weather prediction models: Introduction to the JAS special collection, *J. Atmos. Sci.*, *64*, 3737–3741, doi:10.1175/2007JAS2622.1.

Fetzer, E., et al. (2003), AIRS/AMSU/HSB validation, *IEEE Trans. Geosci. Remote Sens.*, *41*, 418–431, doi:10.1109/TGRS.2002.808293.

Gettelman, A., et al. (2004), Validation of Aqua satellite data in the upper troposphere and lower stratosphere with in situ aircraft instruments, *Geophys. Res. Lett.*, *31*, L22107, doi:10.1029/2004GL020730.

Grell, G. A., and D. Devenyi (2002), A generalized approach to parameterizing convection combining ensemble and data assimilation techniques, *Geophys. Res. Lett.*, *29*(14), 1693, doi:10.1029/2002GL015311.

Halverson, J. B., et al. (2007), NASA's tropical cloud systems and processes experiment: Investigating tropical cyclogenesis and hurricane intensity change, *Bull. Am. Meteorol. Soc.*, *88*, 867–882, doi:10.1175/BAMS-88-6-867.

Hong, S., and J.-O. Lim (2006), The WRF single-moment 6-class microphysics scheme (WSM6), *J. Korean Meteorol. Soc.*, *42*, 129–151.

Hou, A. Y., D. V. Ledvina, A. M. Da Silva, S. Q. Zhang, J. Joiner, and R. M. Atlas (2000), Assimilation of SSM/I-derived surface rainfall and total precipitatble water for improving the GEOS analysis and climate studies, *Mon. Weather Rev.*, *128*, 509–537, doi:10.1175/1520-0493(2000)128<0509:AOSIDS>2.0.CO;2.

Hou, A. Y., S. Q. Zhang, and O. Reale (2004), Variational continuous assimilation of TMI and SSM/I rain rates: Impact on GEOS-3 hurricane analyses and forecasts, *Mon. Weather Rev.*, *132*, 2094–2109, doi:10.1175/1520-0493(2004)132<2094:VCAOTA>2.0.CO;2.

Huffman, G. J., R. F. Adler, D. T. Bolvin, G. Gu, E. J. Nelkin, K. P. Bowman, Y. Hong, E. F. Stocker, and D. B. Wolff (2007), The TRMM Multisatellite Precipitation Analysis (TMPA): Quasi-global, multiyear, combined-sensor precipitation estimates at fine scales, *J. Hydrometeorol.*, *8*, 38–55, doi:10.1175/JHM560.1.

Joiner, J., and D. Dee (2000), An error analysis of radiance and suboptimal retrieval assimilation, *Q. J. R. Meteorol. Soc.*, *126*, 1495–1514, doi:10.1256/smsqj.56513.

Le Marshall, J. F., et al. (2005a), AIRS hyperspectral data improves southern hemisphere forecasts, *Aust. Meteorol. Mag.*, *54*, 57–60.

Le Marshall, J. F., et al. (2005b), AIRS associated accomplishments at the JCSDA–first use of full spatial resolution hyperspectral data show significant improvements in global forecasts, in *Atmospheric and Environmental Remote Sensing Data Processing and Utilization: Numerical Atmospheric Prediction and Environmental Monitoring*, edited by H. Huang et al., *Proc. SPIE*, 5890, 58900O, doi:10.1117/12.615757.

Leslie, L. M., J. F. LeMarshall, R. P. Morison, C. Spinoso, R. J. Purser, N. Pescod, and R. Seecamp (1998), Improved hurricane track forecasting from the continuous assimilation of high quality satellite wind data, *Mon. Weather Rev.*, *126*, 1248–1258, doi:10.1175/1520-0493(1998)126<1248:IHTFFT>2.0.CO;2.

Lorenc, A. C. (1986), Analysis methods for numerical weather prediction, *Q. J. R. Meteorol. Soc.*, *112*, 1177–1194, doi:10.1002/qj.49711247414.

Mlawer, E. J., S. J. Taubman, P. D. Brown, M. J. Iacono, and S. A. Clough (1997), Radiative transfer for inhomogeneous atmosphere: RRTM, a validated correlated-k model for the long-wave, *J. Geophys. Res.*, *102*(D14), 16,663–16,682, doi:10.1029/97JD00237.

Parrish, D. F., and J. C. Derber (1992), The National Meteorological Center's spectral statistical-interpolation analysis system, *Mon. Weather Rev.*, *120*, 1747–1763, doi:10.1175/1520-0493(1992)120<1747:TNMCSS>2.0.CO;2.

Pavelin, E., S. English, and J. Eyre (2008), The assimilation of cloud-affected infrared satellite radiances for numerical weather prediction, *Q. J. R. Meteorol. Soc.*, *134*, 737–749, doi:10.1002/qj.243.

Pu, Z., W.-K. Tao, S. A. Braun, J. Simpson, Y. Jia, J. Halverson, A. Hou, and W. Olson (2002), The impact of TRMM data on mesoscale numerical simulation of supertyphoon Paka, *Mon. Weather Rev.*, *130*, 2448–2458, doi:10.1175/1520-0493(2002)130<2448:TIOTDO>2.0.CO;2.

Pu, Z., X. Li, C. Velden, S. Aberson, and W. T. Liu (2008), Impact of aircraft dropsonde and satellite wind data on the numerical simulation of two landfalling tropical storms during TCSP, *Weather Forecast.*, *23*, 62–79, doi:10.1175/2007WAF2007006.1.

Pu, Z., X. Li, and E. J. Zipser (2009), Diagnosis of the initial and forecast errors in the numerical simulation of rapid intensification of Hurricane Emily, *Weather Forecast.*, *24*, 1236–1251, doi:10.1175/2009WAF2222195.1.

Reale, O., J. Susskind, R. Rosenberg, E. Brin, E. Liu, L. P. Riishojgaard, J. Terry, and J. C. Jusem (2008), Improving forecast skill by assimilation of quality-controlled AIRS temperature retrievals under partially cloudy conditions, *Geophys. Res. Lett.*, *35*, L08809, doi:10.1029/2007GL033002.

Skamarock, W. C., J. B. Klemp, J. Dudhia, D. O. Gill, D. M. Barker, M. G. Duda, X.-Y. Huang, W. Wang, and J. G. Powers (2008), A description of the advanced research WRF version 3, *Tech. Note NCAR/TN-475+STR*, Natl. Cent. for Atmos. Res., Boulder, Colo.

Soden, B. J., C. S. Velden, and E. E. Tuleya (2001), The impact of satellite winds on experimental GFDL hurricane model forecasts, *Mon. Weather Rev.*, *129*, 835–852, doi:10.1175/1520-0493(2001)129<0835:TIOSWO>2.0.CO;2.

Susskind, J., C. Barnet, and J. Blaisdell (2003), Retrieval of atmospheric and surface parameters from AIRS/AMSU/HSB under cloudy conditions, *IEEE Trans. Geosci. Remote Sens.*, *41*, 390–409, doi:10.1109/TGRS.2002.808236.

Tian, B., D. E. Waliser, E. J. Fetzer, B. H. Lambrigtsen, Y. L. Yung, and B. Wang (2006), Vertical moist thermodynamic structure and spatial–temporal evolution of the MJO in AIRS observations, *J. Atmos. Sci.*, *63*, 2462–2485, doi:10.1175/JAS3782.1.

Tobin, C. D., H. E. Revercomb, R. O. Knuteson, B. M. Lesht, L. L. Strow, S. E. Hannon, W. F. Feltz, L. A. Moy, E. J. Fetzer, and T. S. Cress (2006), ARM site atmospheric state best estimates for AIRS temperature and water vapor retrieval validation, *J. Geophys. Res.*, *111*, D09S14, doi:10.1029/2005JD006103.

Velden, C. S., T. L. Olander, and S. Wanzong (1998), The impact of multispectral GOES-8 wind information on Atlantic tropical cyclone track forecasts in 1995. Part 1: Dataset methodology, description and case analysis, *Mon. Weather Rev.*, *126*, 1202–1218, doi:10.1175/1520-0493(1998)126<1202:TIOMGW>2.0.CO;2.

Wu, L. (2009), Comparison of atmospheric infrared sounder temperature and relative humidity profiles with NASA African Monsoon Multidisciplinary Analyses (NAMMA) dropsonde observations, *J. Geophys. Res.*, *114*, D19205, doi:10.1029/2009JD012083.

Wu, L., S. A. Braun, J. J. Qu, and X. Hao (2006), Simulating the formation of Hurricane Isabel (2003) with AIRS data, *Geophys. Res. Lett.*, *33*, L04804, doi:10.1029/2005GL024665.

Zhang, X., Q. Xiao, and P. J. Fitzpatrick (2007), The impact of multisatellite data on the initialization and simulation of Hurricane Lili's (2002) rapid weakening phase, *Mon. Weather Rev.*, *135*, 526–548, doi:10.1175/MWR3287.1.

Z. Pu and L. Zhang, Department of Atmospheric Sciences, University of Utah, 135 S 1460 E, Rm. 819, Salt Lake City, UT 84112, USA. (Zhaoxia.Pu@utah.edu)